Eur Biophys J (2003) 32: 60–66
DOI 10.1007/s00249-002-0268-5

ARTICLE

Armando Carpaneto

Nickel inhibits the slowly activating channels of radish vacuoles

Received: 1 August 2002 / Revised: 21 October 2002 / Accepted: 24 October 2002 / Published online: 9 January 2003
© EBSA 2003

Abstract The mechanism of inhibition by cytoplasmic nickel of slowly activating channels in radish vacuoles was investigated using the patch-clamp technique. The decrease in the macroscopic current induced by the presence of nickel in the cytoplasmic solution can be described by a Michaelis-Menten equation with an apparent dissociation constant of 0.45 ± 0.03 mM. At the single-channel level, nickel moderately decreases the single-channel conductance, since the ratio between the chord conductance in the presence and in the absence of 1 mM cytosolic nickel is 0.89 ± 0.06. Experiments performed to study the interaction between calcium, an activator of the channel, and nickel strongly suggest that these two ions bind to two distinct molecular sites. A simple mathematical model predicting the experimental observations is presented.

Keywords Divalent ions · Plant ion channels · Radish vacuoles

Introduction

Slowly activating channels (Hedrich and Neher 1987), usually referred to as slow vacuolar (SV) channels or SV channels, mediate a large part of the ionic current of tonoplasts in all plant species investigated so far (Allen and Sanders 1997). These channels are regulated by a variety of chemico-physical parameters such as membrane voltage, cytoplasmic magnesium (Carpaneto et al. 2001; Pei et al. 1999), reducing and oxidizing agents (Bertl and Slayman 1990; Carpaneto et al. 1999), both cytoplasmic and vacuolar calcium as well as pH (Hedrich and Neher 1987; Pottosin et al. 1997). The SV channels are blocked by compounds such as ruthenium red (Pottosin et al. 1999), 14-3-3 proteins (Van den Wijngaard et al. 2001), polyamines (Dobrovinskaya et al. 1999), zinc (Schulz-Lessdorf and Hedrich 1995) and nickel (Paganetto et al. 2001). Through the pore of the SV channel, both monovalent (such as K^+, Na^+) and divalent (such as Ca^{2+} and Mg^{2+}) cations can permeate (Pottosin et al. 2001). Mathematical models for the permeation (Allen et al. 1998) and for the gating (Carpaneto 2001; Carpaneto et al. 2001) of the SV channel have been proposed. Though these channels have been intensively studied, their physiological role is still unclear (Pottosin et al. 1997; Ward and Schroeder 1994). An electrophysiological characterization of slow vacuolar channels in radish vacuoles has already been performed (Gambale et al. 1993) using the patch-clamp technique; here the blocking effects of cytoplasmic nickel were analysed and this divalent ion was used as a tool to identify the presence of different binding sites for electrically charge cations in the protein structure. Moreover, large amounts of metals are present in the environment. When absorbed by plants, they can be transferred to humans, causing toxicity and affecting a variety of physiological processes. Therefore these studies may be useful, both to clarify the microscopic mechanisms controlling the interaction between the membrane channels and divalent cations, and for a general, more integrated, point of view.

Materials and methods

Radish plants (*Raphanus sativus* cv, round red outdoor) were grown in the field. Vacuoles were directly extruded into the petri dish by cutting a slice of fresh taproot tissue and rinsing the surface with a few drops of bathing solution. Their ionic transport properties were studied using the patch-clamp technique in the whole-vacuole or the (cytoplasmic side out) excised-patch configuration. Access to the vacuole interior was gained by breaking the membrane under the patching pipette with a short (~1 ms) voltage pulse up to ~1 V. Transmembrane voltages and ionic currents were controlled and monitored with a List EPC7 current-voltage amplifier interfaced with an Instrutech A/D/A board (Instrutech,

A. Carpaneto
Istituto Biofisica, Genova, C.N.R.,
Via De Marini 6, 16149 , Genova, Italy
E-mail: carpaneto@icb.ge.cnr.it
Fax: +39-(0)106475500

Elmont, N.Y., USA). The current and voltage convention was in accordance with Bertl et al. (1992), i.e. the potential difference across the vacuolar membrane, V, is calculated as $V = V_{cytosol} - V_{vacuole}$. This convention implies that positive currents represent cations which flow out of the cytosol and enter the vacuole. The standard solutions were identical in the pipette and in the bath, i.e. (in mM) 200 KCl, 5 $MgCl_2$, 25 MES, 1 $CaCl_2$. The pH of both solutions was adjusted to 6.4 by the addition of KOH. In the external (cytosolic) solution, calcium was varied from 0.1 to 10 mM and nickel was added up to 10 mM. The cytoplasmic solution was changed using a perfusion system based on (up to) 12 polyethylene tubes respectively filled with the standard bath solution (1 mM calcium, no nickel) and the solutions to be investigated. Each tube was alternately adjusted in front of the vacuole for a few seconds by a hydraulic manipulator. The flow in each tube was driven by gravity and regulated by a "phleboclysis" type system at a speed of less than 20 mL/h. The level of the bath solution in the recording chamber was kept constant using a peristaltic pump.

The access resistance (R_a) in the whole-vacuole measurements was in the order of 2–10 MΩ; data were systematically discarded if $|I_{effect} - I_{stand}| R_a > 5$ mV, where I_{stand} was the current recorded in standard solutions and I_{effect} the current recorded on varying $[Ca^{2+}]$ or adding $[Ni^{2+}]$ to the cytosolic solution. Data analysis was done by home-made programs using Igor (Wavemetrics, Lake Oswego, Ore., USA); all data points are given as mean ± standard deviation and are the result of at least three different measurements.

Results

When added to the cytoplasmic solution, nickel acted as an inhibitor of slowly activating channels in radish vacuoles. In Fig. 1A (left), currents were recorded at a voltage of +100 mV in the absence (control recovery) or in the presence of different concentrations of nickel; it can be observed that 10 mM of cytoplasmic nickel completely and reversibly blocked the channels. Figure 1A (right) summarizes the difference in the *I-V* characteristics observed under control conditions (empty symbols) or in the presence of 1 mM cytosolic Ni^{2+} (filled squares). A thorough analysis of the effect of nickel as a function of the applied voltage was prevented by the fact that, in the voltage range investigated, the SV channel conductance was far from reaching saturation; however, the ratio (I_{nor}) between the current recorded in the presence and in the absence of cytosolic Ni^{2+} did not depend on the voltage up to +100 mV (data not

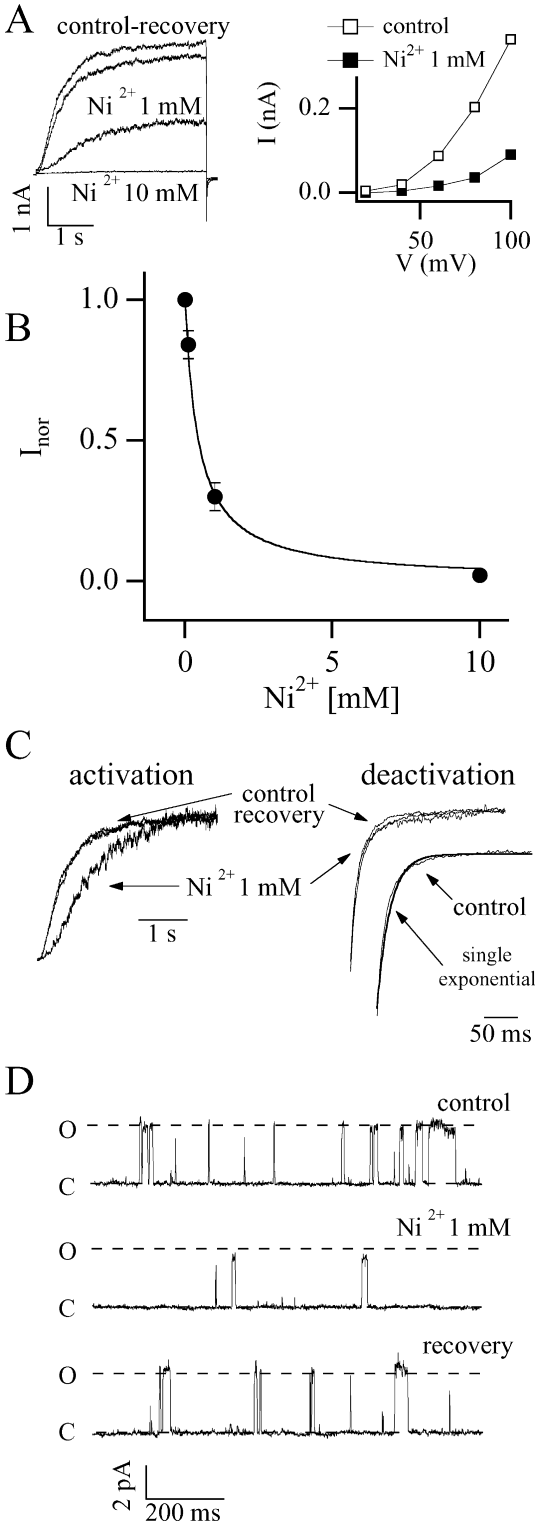

Fig. 1A–D Inhibition of the SV current by cytoplasmic Ni^{2+}. **A** Macroscopic currents (*left*) recorded in the absence (control) or in the presence of 1 or 10 mM nickel. The recovery trace in the absence of $[Ni^{2+}]$ demonstrates that the inhibition induced by nickel is reversible. Voltage stimulation to +100 mV from a holding potential of 0 mV. Tail voltage of −100 mV. *Right*: *I-V* characteristics, from a different experiment, without and with 1 mM Ni^{2+}. **B** Normalized current, I_{nor}, representing the ratio between the current recorded in the presence and in the absence of nickel as a function of $[Ni^{2+}]_{cyt}$. The experimental data can be described using a Michaelis-Menten equation with a K_m equal to 0.45 ± 0.03 mM. The experimental points were recorded at +100 mV. **C** The activation and the deactivation time under control conditions and in the presence of 1 mM Ni^{2+} were compared by scaling the currents at the same stationary value. The recovery currents represent the reversibility of the nickel effect. Activation and deactivation voltages respectively of +100 and −100 mV. In the *inset*, on the *right*, the control current was approximated by a single exponential function. **D** Single-channel recordings in the absence (control recovery) and in the presence of 1 mM nickel added to the cytoplasmic solution. Slow vacuolar channels in radish vacuoles show a main chord conductance of about 120 pS which is slightly affected by the presence of nickel. C and O represent the closed and open states, respectively. Applied voltage: +30 mV. Data were sampled at 2 kHz and filtered at 500 Hz

shown). If I_{nor} was plotted as a function of Ni^{2+} (Fig. 1B), the experimental points could be fitted by the Michaelis-Menten equation, $K_m/(K_m+[Ni^{2+}])$, with an apparent dissociation constant (K_m) equal to 0.45 ± 0.03 mM. The kinetic properties of the channel were also affected by cytosolic nickel, as shown by the slower activation time of the current recorded in 1 mM Ni^{2+} with respect to the control current (see Fig. 1C, left). Interestingly, nickel had no effect on the deactivation time course (Fig. 1C, right).

At the single-channel level (Fig. 1D), nickel slightly decreased the chord single-channel conductance (γ); at $V=+30$ mV in the presence of 1 mM cytosolic nickel, $\gamma_{[Ni2+]}=99.2\pm0.4$ pS (n = number of channels, $n=30$), while in the absence of nickel, $\gamma_{control}=112.2\pm6.8$ pS ($n=230$). The ratio between the two chord conductances was 0.89 ± 0.06. Experiments were performed by varying the cytoplasmic calcium concentrations in the absence or in the presence of 1 mM cytoplasmic nickel. The values of the currents (I_{nor}), normalized to the control current recorded at 1 mM $[Ca^{2+}]_{cyt}$ and in the absence of $[Ni^{2+}]_{cyt}$, are plotted against calcium in Fig. 2A. In the absence of nickel, the increase in calcium concentration (open symbols) activated the slow vacuolar channels, reaching a saturation value between 3 and 5 mM calcium. When 1 mM nickel was added to the extravacuolar solution (filled symbols), the normalized current still saturated at calcium concentrations between 3 and 5 mM, but its value was significantly lower than the corresponding value recorded in the absence of nickel. This experimental evidence strongly suggests the presence of different binding sites for calcium and nickel. The experimental data in Fig. 2A can be successfully approximated (continuous lines) using the Hill equation:

$$I_{nor}=\frac{I_{sat}}{1+\left(\frac{K_h}{[Ca^{2+}]_{cyt}}\right)^n} \quad (1)$$

The same parameters ($K_h=0.86\pm0.03$ and $n=2.7\pm0.1$, resulting from the fit of experimental points in the absence of nickel) were also used to fit the data recorded in the presence of 1 mM $[Ni^{2+}]_{cyt}$; the values of I_{sat} in the absence and in the presence of $[Ni^{2+}]_{cyt}$ were 1.7 ± 0.1 and 0.66 ± 0.04, respectively. The slight deflection observed in Fig. 3 with 10 mM calcium could be due to a decrease of the single-channel conductance at this high calcium concentration (Pei et al. 1999; Pottosin et al. 1997); this phenomenon has not been characterized here and did not alter the conclusion drawn in this paper. Finally, besides increasing the currents, cytosolic calcium increases both the activation and the deactivation time, as shown in Fig. 2B.

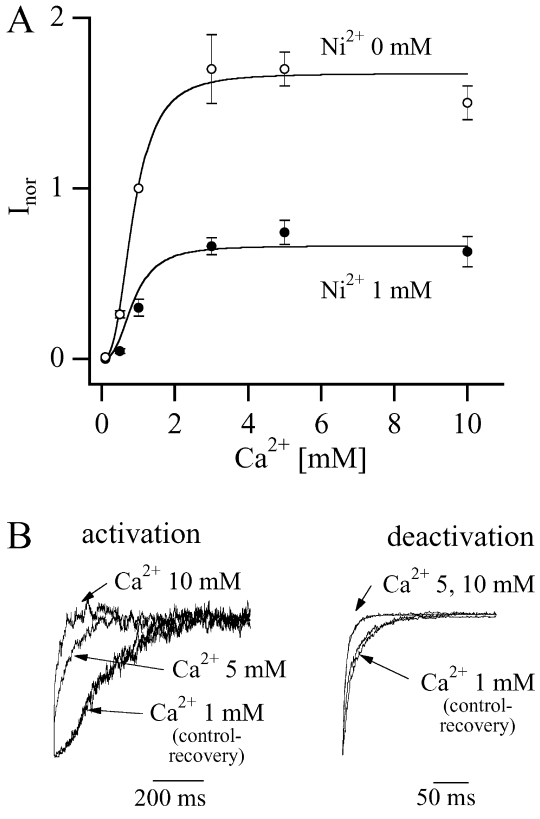

Fig. 2A, B Non-competitive interaction between calcium and nickel in the slow vacuolar channels from radish vacuoles. **A** The values of the currents (I_{nor}) normalized to the control current recorded at 1 mM $[Ca^{2+}]_{cyt}$ and in the absence of $[Ni^{2+}]_{cyt}$ are displayed against calcium concentration. The *continuous lines* represent the fitting of experimental points with Hill equations that have the same K_h and n values (see Results). Applied voltage: +100 mV. **B** Currents in different $[Ca^{2+}]_{cyt}$ normalized at the same stationary value. It can be observed that the deactivation currents at 5 or 10 mM Ca^{2+} are indistinguishable. Activation and deactivation voltages of +100 and −100 mV, respectively

Discussion

Slowly activating channels in radish vacuoles have similar biophysical characteristics to analogous channels in other plant species (Carpaneto et al. 1997; Gambale et al. 1996; Paganetto et al. 2001). By studying the effect of cytoplasmic magnesium, an activator of SV channels, Pei et al. (1999) have suggested the presence of two cytosolic binding sites, one with a high affinity for cytosolic calcium and the other with a low affinity both for cytosolic calcium and magnesium. In this paper, using nickel as a molecular tool we provide evidence of a binding site for divalent ions in the SV channel that is independent of cytoplasmic calcium; nickel binding at this site can be described by a simple Michaelis-Menten mechanism with $K_m=0.45\pm0.03$. The fact that nickel did not significantly affect the single-channel conductance suggests that the part of the protein site interacting with Ni^{2+} is far from the channel's selectivity filter. Moreover, in the presence of nickel, even the highest concentrations of cytoplasmic calcium used (up to 10 mM) are unable to relieve nickel inhibition. The saturation values obtained in the absence and in the presence of nickel for high levels of cytosolic calcium are significantly different (see Fig. 3); this indicates a

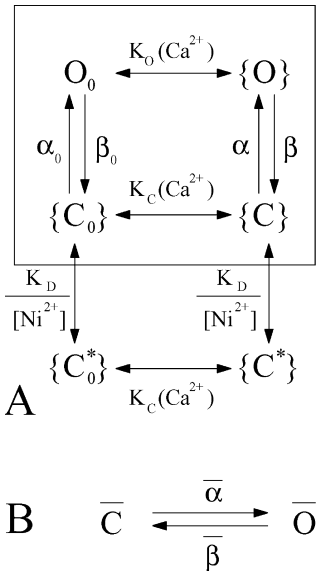

Fig. 3 A Gating scheme allowing the binding of one nickel ion to the channel (see Appendix). The interaction of the channel with calcium is represented schematically inside the box. **B** Under the conditions discussed in the Appendix, the gating scheme shown in **A** can be reduced to a simple two-state system

non-competitive interaction between calcium and nickel. Non-competitive inhibition caused by nickel is also supported both by the satisfactory match between experimental data and the Hill plots shown in Fig. 3 and by the different effects induced by Ni^{2+} and Ca^{2+} on the deactivation time course (Figs. 1C and 2B, right traces). It must be observed that a Hill coefficient of about 3 would indicate a cooperative interaction of at least three calcium ions with the protein. In sugar beet vacuoles, Hedrich and Neher (1987) found a value near to 1. This difference could be ascribed either to the different calcium concentration range investigated (Hedrich and Neher worked up to 0.1 mM cytosolic calcium) or to a difference in the channel structure, possibly due to the fact that these authors used a different plant.

All the experimental findings, the stationary nickel block (Fig. 2A, B), the non-competitive interaction between nickel and calcium (Fig. 2A) and the kinetics of the binding of nickel and calcium to the channel (Figs. 1C and 2B) can be described by the model proposed in Fig. 3. A detailed description of the model and the ability of the kinetic scheme to account for the experimental evidence are illustrated in the Appendix. The model assumes that nickel can only bind to the closed states with a dissociation constant K_D which is independent of the presence or absence of calcium bound to the channel. It is worth noting that if we assume a less strict condition, i.e. that nickel can bind to the channel without preference for any of its conformations (eight-state model), the open probability can be obtained by a simple equation:

$$P\left(V, Ca^{2+}, Ni^{2+}\right) = P\left(V, Ca^{2+}, 0\right) \times \left(1 + \left[Ni^{2+}\right]/K_m\right)^{-1} \quad (2)$$

The model can describe all stationary data, but, clearly, as rate constants are nickel independent, fails to predict the increase in the time course of activation due to nickel binding (Fig. 1C, left panel).

These results could be useful for a more complete characterization of the functional and structural properties of the SV channel, an ubiquitous channel that is present in all plants investigated so far. Interestingly, Paganetto et al. (2001) found that, under identical experimental conditions, the SV channel displayed different nickel sensitivities in sugar beet and water hyacinth, as K_m was 24.8 ± 2.0 μM for sugar beet and 98.7 ± 20.0 μM for water hyacinth. In radish vacuoles used in our study, we found a higher K_m value of 0.45 ± 0.03 mM. Owing to differences in experimental conditions, it is difficult to compare the data from the two papers; as a matter of fact, the cytosolic potassium concentration and the value of cytosolic pH were $[K^+] = 200$ mM and pH = 6.4 in our study and $[K^+] = 150$ mM and pH = 7.0 in the work of Paganetto et al. (2001). Increasing the cytosolic potassium concentration decreases the binding of heavy metals to ion channels, possibly by direct competition or by a screening effect induced by K^+ on the heavy-metal binding site (for a more comprehensive discussion, see Bregante et al. 1997). As far as cytoplasmic proton concentration is concerned, one may speculate that, from a molecular point of view, histidines in the channel could be responsible for nickel binding. In that case a decrease in pH increases nickel solubility, resulting in a lower affinity of the channel's binding site for nickel (Smith and Martell 1989). Taken together, all these observations indicate that the interaction between heavy metals and plants might depend on a series of parameters linked to the state of the plant itself (for example, the cytosolic potassium concentration). However, we cannot exclude that the channel itself has a different sensitivity to nickel with respect to the corresponding counterparts in sugar beet and water hyacinth. Although radish (*Raphanus sativus*) is not a metal accumulator (Bernal and McGrath 1994), this plant belongs to the family of *Cruciferae* and several species in this family (for example, *Brassica juncea*, *Alyssum bertolonii*, *Thlapsi caerulescens*) are well known for their metal tolerance/accumulation capability (Salt et al. 1998).

There is a lack of data on nickel concentration in the plant cytosol which makes it difficult to correlate the nickel concentrations used in this study with physiological (or toxic) levels of Ni^{2+}. However, the K_m obtained in this study and in the work of Paganetto et al. (2001) might represent an upper limit for cytosolic nickel concentration; above this level, Ni^{2+} might have dramatic effects on plant growth and survival. Indeed, it has been demonstrated that the nickel concentration for half inhibition of growth in radish seeds is 0.2 mM (Espen et al. 1997), i.e. comparable to the K_m concentration acting on the slow vacuolar radish channel. Moreover, it has also been demonstrated (Espen et al. 1997) that in

radish seeds this inhibitory process induced by Ni^{2+} affects potassium transport and distribution and cannot be reversed by comparable calcium concentrations. Intriguingly, one may speculate that the absence of competition between calcium and nickel and the critical concentrations for growth inhibition in radish seeds may be related to the effects on radish slow vacuolar currents reported in this paper.

Since pollution of the biosphere with heavy metals poses major environmental and human health problems (Salt et al. 1998), the interaction between metals and plant transport proteins is an emerging theme both from the point of view of food quality and for future plans where plants could be used in phytoremediation systems for the decontamination of metal-polluted soils or waters.

Acknowledgements The author wishes to thank F. Gambale for his valuable help and useful discussions throughout this study, P. Magistrelli for interesting comments on the paper and S. de Robertis for English language assistance.

Appendix

Model description

By analogy to calcium-activated BK channels (Cui et al. 1997), we schematize the voltage and calcium dependence of the SV channels with the gating scheme in the box in Fig. 3A. We assume that calcium binding to the channel (indicated with a single double-headed arrow) is faster than the voltage-dependent gating (indicated with two arrows). $\{C_0\}$ and O_0 respectively represent the set of possible closed states and the open state (one single open state is justified by the single decaying exponential; see Fig. 1C, right) of the SV channel when it does not bind any calcium ion. $\{C\}$ and $\{O\}$ are the set of possible closed and open states of the SV channel when it binds from one to at least three calcium ions. The voltage-dependent rate constants are represented by α_0, β_0, α and β, while $K_C(Ca^{2+})$ and $K_O(Ca^{2+})$ are the calcium-dependent association constants for the closed and open states, respectively; when $[Ca^{2+}]=0$ then $K_C(0)=K_O(0)=0$. The fact that the time course of activation increases in the presence of nickel (Fig. 1C, left panel) suggests that nickel can bind to the channel only if the channel is in the closed configuration (see also Discussion and the section Activation and deactivation time, below); as for calcium, nickel binding (indicated in Fig. 3A with a single double-headed arrow) is faster than the voltage-dependent gating. The asterisks indicate that the channel in that conformational state has bound a single nickel ion. K_D is the calcium-independent Ni^{2+} dissociation constant for the states $\{C^*_O\}$ and $\{C^*\}$. In the absence of experimental evidence, $K_C(Ca^{2+})$, $K_O(Ca^{2+})$ and K_D are assumed to be voltage independent.

The channel opening probability of the scheme in Fig. 3A is:

$$P\left(V,Ca^{2+},Ni^{2+}\right)=\frac{1}{1+\frac{\beta_0(V)}{\alpha_0(V)}\frac{K_C\left(Ca^{2+}\right)}{K_O\left(Ca^{2+}\right)}\left(1+\frac{\left[Ni^{2+}\right]}{K_D}\right)} \quad \text{(A1)}$$

The microscopic reversibility applied to the loop in the box of Fig. 3A requires that $\frac{\beta}{\alpha}=\frac{\beta_0}{\alpha_0}\frac{K_C}{K_O}$. As, in SV channels, calcium shifts the open probability towards negative potential, this means that $\frac{K_C}{K_O}<1$, i.e. calcium has more affinity to the open than to the closed state. Under this hypothesis we show that the kinetic scheme of Fig. 3A can predict the experimental findings presented in this paper.

Nickel binding to the SV channel

If we neglect the single-channel conductance block induced by nickel, we can write, in agreement with Fig. 1B:

$$\frac{P\left(V,Ca^{2+},Ni^{2+}\right)}{P\left(V,Ca^{2+},0\right)}=\frac{1}{1+\frac{\left[Ni^{2+}\right]}{K_m}} \quad \text{(A2)}$$

where:

$$P\left(V,Ca^{2+},0\right)=\frac{1}{1+\frac{\beta_0}{\alpha_0}\frac{K_C}{K_O}} \quad \text{(A3)}$$

From Eqs. (A1) and (A2) it is easy to obtain a relation between the apparent and real dissociation constants, K_m and K_D:

$$K_m=\frac{1+A}{A}K_D \quad \text{(A4)}$$

where $A=\frac{\beta_0}{\alpha_0}\frac{K_C}{K_O}$. This equation says that: (1) $K_D \le K_m < \frac{1+A}{A}K_D$; (2) even if K_D is independent of the applied voltage, K_m should present voltage dependence. However, for voltages in which the open probability is small (i.e. in our experimental conditions), the parameter A must be greater than 1 and Eq. (A4) predicts that K_m is a good estimation of K_D.

Non-competitive inhibition induced by nickel

In the voltage range investigated and for every nickel concentration, in the absence of cytosolic calcium we could not record any channel activity; this implies that $\beta_0 \gg \alpha_0$. On the other hand, when $[Ca^{2+}] \to +\infty$ then:

$$P\left(V,\infty,Ni^{2+}\right)=\frac{1}{1+\frac{\beta_0}{\alpha_0}\frac{K_C(\infty)}{K_O(\infty)}\left(1+\frac{\left[Ni^{2+}\right]}{K_D}\right)} \quad \text{(A5)}$$

From data presented in Fig. 2A we can write:

$$\frac{P\left(V,Ca^{2+},Ni^{2+}\right)}{P\left(V,\infty,Ni^{2+}\right)}=\frac{1}{1+\left(\frac{K_h}{\left[Ca^{2+}\right]}\right)^3} \quad \text{(A6)}$$

Equation (A6) is not verified for every $[Ca^{2+}]$ but we can impose that it is true for $[Ca^{2+}]=K_h$. After some calculations we obtain:

$$\frac{K_C(K_h)}{K_O(K_h)}=\frac{1}{\frac{\beta_0}{\alpha_0}\left(1+\frac{[Ni^{2+}]}{K_D}\right)}+2\frac{K_C(\infty)}{K_O(\infty)} \quad (A7)$$

On the right-hand side the first term tends to zero (as $\beta_0 \gg \alpha_0$); therefore K_h is nickel independent, as expected for non-competitive inhibition.

Activation and deactivation time

Let us assume that both the activation and the deactivation time courses can be described by single exponential functions (this is only true for the deactivation process); then the closed states without calcium are represented by a single state. The gating scheme of Fig. 3A can be reduced to the scheme in Fig. 3B, imposing that $\bar{C}=C_0+\{C\}+C_0^*+\{C^*\}$ and $\bar{O}=O_0+\{O\}$. The following relationships are valid:

$$\bar{C}+\bar{O}=1 \quad (A8)$$

$$\{C\}=K_C(Ca^{2+})C_0 \quad (A9)$$

$$\{O\}=K_O(Ca^{2+})O_0 \quad (A10)$$

$$\frac{\{C^*\}}{\{C\}}=\frac{C_0^*}{C_0}=\frac{[Ni^{2+}]}{K_D} \quad (A11)$$

After some calculations we obtain:

$$\bar{\alpha}=\frac{\alpha_0+K_C(Ca^{2+})\alpha_1}{(1+K_C(Ca^{2+}))\left(1+\frac{[Ni^{2+}]}{K_D}\right)} \quad (A12)$$

$$\bar{\beta}=\frac{\beta_0+K_O(Ca^{2+})\beta_1}{1+K_O(Ca^{2+})} \quad (A13)$$

The time constant, τ, is therefore $\tau=\frac{1}{\bar{\alpha}+\bar{\beta}}$. Of course, for positive voltages the time constant will be $1/\bar{\alpha}$, while τ will approach $1/\beta$ for negative transmembrane potentials. Therefore an increase of Ni^{2+} will result in an increase of τ (slower activation) at positive voltages and will not affect the deactivation process (β is independent of Ni^{2+}). On the other hand, both activation and deactivation process will be affected by calcium. As an increase of calcium induces a decrease of τ at positive voltages, we must impose that α_1 is greater than α_0. For the same reason, at negative voltages, $\beta_1/\beta_0>1$; using the principle of microscopic reversibility we obtain that $\frac{\alpha_1}{\alpha_0}>\frac{K_O}{K_C}$. We are reminded that $K_O>K_C$ is necessary to shift $P(V, Ca^{2+}, Ni^{2+})$ toward more negative potentials. It is interesting to note that if $K_O>K_C$, $\alpha_1>\alpha_0$ but $\frac{\alpha_1}{\alpha_0}<\frac{K_O}{K_C}$ then the deactivation process would be slower increasing calcium in the cytosol, a condition experimentally observed for BK channels (Cui et al. 1997).

References

Allen GJ, Sanders D (1997) Vacuolar ion channels. Adv Bot Res 25:217–252

Allen GJ, Sanders D, Gradmann D (1998) Calcium-potassium selectivity: kinetic analysis of current-voltage relationship of the open slowly activating channel in the vacuolar membrane of *Vicia faba* guard-cells. Planta 204:528–541

Bernal MP, McGrath SP (1994) Effects of pH and heavy metal concentrations in solution culture on the proton release, growth and elemental composition of *Alyssum murale* and *Raphanus sativus L.* Plant Soil 166:83–92

Bertl A, Slayman CL (1990) Cation-selective channels in the vacuolar membrane of *Saccharomyces*: dependence on calcium, redox state, and voltage. Proc Natl Acad Sci USA 87:7824–7828

Bertl A, Blumwald E, Coronado R, Eisenben R, Firlay G, Gradmann D, Hille B, Kohler K, Koll HA, MacRobbie E, Meissner G, Miller C, Neher E, Palade P (1992) Electrical measurements on endomembranes. Science 258:873–874

Bregante M, Carpaneto A, Pastorino F, Gambale F (1997) Effects of mono- and multi-valent cations on the inward-rectifying potassium channel in isolated protoplasts from maize roots. Eur Biophys J 26:381–391

Carpaneto A (2001) A cyclic model for bimodal activation of calcium activated potassium channels in radish vacuoles. Riv Biol 94:83–104

Carpaneto A, Cantù AM, Busch H, Gambale F (1997) Ion channels in the vacuoles of the seagrass *Posidonia oceanica*. FEBS Lett 412:236–240

Carpaneto A, Cantù AM, Gambale F (1999) Redox agents regulate ion channel activity in vacuoles from higher plant cells. FEBS Lett 442:129–132

Carpaneto A, Cantù AM, Gambale F (2001) Effects of cytoplasmic Mg^{2+} on slowly activating channels in isolated vacuoles of *Beta vulgaris*. Planta 213:457–468

Cui J, Cox DH, Aldrich RW (1997) Intrinsic voltage dependence and Ca^{2+} regulation of *mslo* large conductance Ca-activated K^+ channels. J Gen Physiol 109:647–673

Dobrovinskaya OR, Pottosin II, Muniz J (1999) Inhibition of vacuolar ion channels by polyamines. J Membr Biol 167:127–140

Espen L, Pirovano L, Cocucci SM (1997) Effects of Ni^{2+} during the early phases of radish (*Raphanus sativus*) seed germination. Environ Exp Bot 38:187–197

Gambale F, Cantù AM, Carpaneto A, Keller BU (1993) Fast and slow activation of voltage-dependent ion channels in radish vacuoles. Biophys J 65:1837–1843

Gambale F, Bregante M, Stragapede F, Cantù AM (1996) Ionic channels of the sugar beet tonoplast are regulated by a multi-ion single-file permeation mechanism. J Membr Biol 154: 69–79

Hedrich R, Neher E (1987) Cytoplasmic calcium regulates voltage-dependent ion channels in plant vacuoles. Nature 329:833–835

Paganetto A, Carpaneto A, Gambale F (2001) Ion transport and metal sensitivity of vacuolar channels from the roots of the aquatic plant *Eichhornia crassipes*. Plant Cell Environ 24:1329–1336

Pei ZM, Ward JM, Schroeder JI (1999) Magnesium sensitizes slow vacuolar channels to physiological cytosolic calcium and inhibits fast vacuolar channels in fava bean guard cell vacuoles. Plant Physiol 121:977–986

Pottosin II, Tikhonova LI, Hedrich R, Schönknecht G (1997) Slowly activating vacuolar channels cannot mediate Ca^{2+}-induced Ca^{2+} release. Plant J 12:1387–1398

Pottosin II, Dobrovinskaya OR, Muniz J (1999) Cooperative block of the plant endomembrane ion channel by ruthenium red. Biophys J 77:1973–1979

Pottosin II, Dobrovinskaya OR, Muniz J (2001) Conduction of monovalent and divalent cations in the slow vacuolar channel. J Membr Biol 181:55–65

Salt DE, Smith RD, Raskin I (1998) Phytoremediation. Annu Rev Plant Physiol Plant Mol Biol 49:643–668

Schulz-Lessdorf B, Hedrich R (1995) Protons and calcium modulate SV-type channels in the vacuolar-lysosomal compartment – channel interaction with calmodulin inhibitors. Planta 197:655–671

Smith R, Martell AE (1989) Critical stability constants, vol 6. Plenum Press, New York

Van den Wijngaard P, Bunney T, Roobeek I, Schonknecht G, De Boer A (2001) Slow vacuolar channels from barley mesophyll cells are regulated by 14-3-3 proteins. FEBS Lett 488:100–104

Ward JM, Schroeder JI (1994) Calcium-activated K^+ channels and calcium-induced calcium release by slow vacuolar ion channels in guard cell vacuoles implicated in the control of stomatal closure. Plant Cell 6:669–683